

# Thermal analysis of a solar air heater for drying purposes

Z.Deniz ALTA<sup>1</sup>, Nuri ÇAĞLAYAN<sup>2\*</sup>, Mehmet Akif EZAN<sup>3</sup>, Can ERTEKİN<sup>1</sup>

(1. Department of Farm Machinery, Faculty of Agriculture, Akdeniz University, 07058 Antalya – Turkey;

2. Technical Sciences of Vocational Training School, Akdeniz University, 07058 Antalya – Turkey;

3. Department of Mechanical Engineering, Dokuz Eylül University, Buca, 35397 İzmir – Turkey. )

**Abstract:** In this study, energetic efficiency of a solar air heater with aluminum flat plate absorber was examined experimentally for airflow velocity of 2, 3 and 4 m/s. An experimental setup was built-up and experiments were compared with the results of the analysis performed by using computational fluid dynamics (CFD) software. Results were also evaluated based on thermographic camera images.

**Keywords:** Solar air heater, energy efficiency, absorber plate

**Citation:** Alta, Z. D., N. Çağlayan, M. A. Ezan, and C. Ertekin. 2015. Thermal analysis of a solar air heater for drying purposes. *Agric Eng Int: CIGR Journal*, Special issue 2015: 18th World Congress of CIGR: 193-199.

## 1 Introduction

The solar energy collection as a renewable energy resource has been the primary interest of many engineers and researchers for the last two centuries due to its widespread applications (Selmi et al., 2008). In this context, solar air heaters are implemented in many different practices, which require low to moderate temperatures below 60°C (Esen, 2008). They are generally used for space heating, drying for industrial & agriculture purposes (Gupta and Kaushik, 2008). The main disadvantage of solar air heaters is possessing lower thermal efficiency in consequence of inherently low heat transfer capability between the absorber plate and air flowing in the duct (Kumar and Saini, 2009). On the other hand, the most important advantages for air-type solar heaters include: no freezing, boiling or pressure problems; generally lower weight and low construction cost (Selcuk, 1977).

Computational fluid dynamics (CFD) is used as powerful simulation technique to observe the collector efficiency with less time and cost consuming in recent

years. Many experimental studies have been carried out to evaluate performance of solar air heaters but very few attempts of CFD investigation have been made so far due to complexity of flow pattern and computational limitations (Yadav and Bhagoria, 2013; Wang et al., 2006). With the development of computer, hardware and numerical methodology, applications of CFD are being used to carry out critical investigations in the field of solar air heaters.

The work presented in this paper aims to analyze the heat exchange process inside the solar air heater and evaluate the energy efficiency.

## 2 Material and method

The experimental setup and schematic diagram of the solar air heater was shown in Figure 1. In addition, the design parameters of the heater are summarized in Table 1. A single glazing was chosen in order to maximize the radiation impact on the absorber and reduce convective losses. Dimensions of the air heater are 1.92 x 0.82 x 0.10 m, in length, width and height, respectively. The heater has an insulation thickness of 0.05 m on the bottom and lateral surfaces. The gap between the absorber plate and bottom of the heater is 0.043 m. The thickness of the

Received date: 2014-12-02

Accepted date: 2015-01-07

\*Corresponding author: Nuri ÇAĞLAYAN, Technical Sciences of Vocational Training School, Akdeniz University, 07058 Antalya – Turkey. Email: nuricaglayan@akdeniz.edu.tr

absorber plate is 2 mm and its surface is painted matt black.

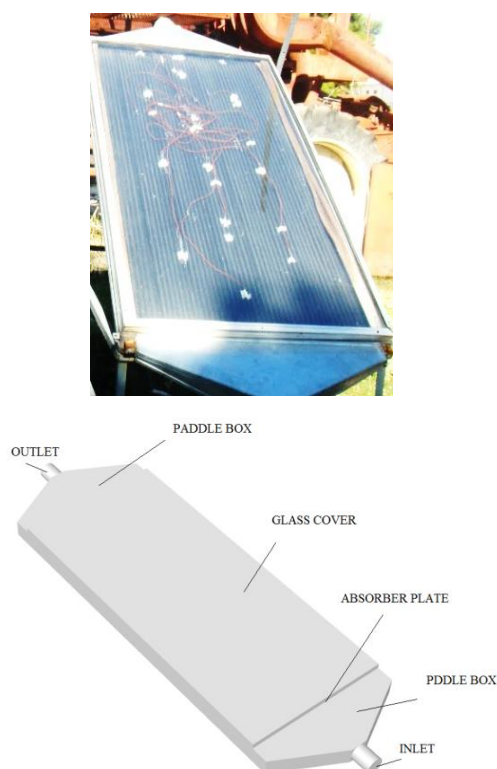


Figure 1 Experimental setup and the cross section of the solar air heater

**Table1 Main properties solar air heater**

Parameters	Value
Absorber material	Aluminum
Plate thickness	2 mm
Absorber coating	Dull black paint
Glazing	Single glass (thickness 4 mm)
Workingfluid in flow ducts	Air
Width of the duct, W	0.82 m
Collector side wall height, $h_c$	0.1 m
Air flow duct height, D	43 mm
Length of the collector, L	1.9 m
Emissivity of the glass cover, $\varepsilon_g$	0.85
Emissivity of the absorber plate, $\varepsilon_p$	0.95
Emissivity of the bottom plate, $\varepsilon_b$	0.95
Tilt angle, $\beta$	35°
Insulation thicknesses, $t_b, t_c$	50 mm
Thermal conductivity of insulation, $\lambda$	0.043 W/m.K
Heat transfer coefficient of aluminum, $\lambda_{Al}$	210 W/m.K
Heat capacity of aluminum, $c_{p,Al}$	0.90 J/g.°C

In this study, inlet and outlet air temperatures of solar air heater, ambient temperature, airflow rate, solar radiation, pressure drop and wind velocity was measured and all of data were recorded by a data logger. A radial fan with a capacity of 0.41 m<sup>3</sup>/s was used for solar air heater to provide the airflow. A controller unit was used to adjust the fan speed and airflow rate.

Inlet and outlet air temperature, absorber plate surface and ambient temperature were measured by using K-type thermocouples. Wind speed was measured using a cup anemometer (Delta-T A100 R, accuracy: 1%  $\pm$ 0.1 m/s). Anemometer was placed about 1 m above the solar air heater. A flow meter [Testo 405, accuracy: ( $\pm$ 0.1 m/s  $\pm$ 5% of m.v.) at 0-2 m/s and ( $\pm$ 0.3 m/s  $\pm$ 5% of m.v.) at 2.01-10 m/s] was used to measure the inlet air velocity for the solar air heater. The amount of global incident solar radiation on the heater was measured using a solar sensor (Delta-T ES2, accuracy:  $\pm$ 3% at 20°C). The solar sensor was placed on the glass cover of the heater. All of sensors were connected to a data logger (Delta-T, DL2e) and the measurements were recorded 5 min interval.

### 3 Results

Figure 2 presents a typical day for solar radiation, inlet and outlet air temperatures between 09.00 am and 04.00 pm. The ambient temperature was considered to be the same as the inlet air temperature. It seems that inlet, outlet air temperatures increase with increasing solar radiation and the highest values were observed at midday.

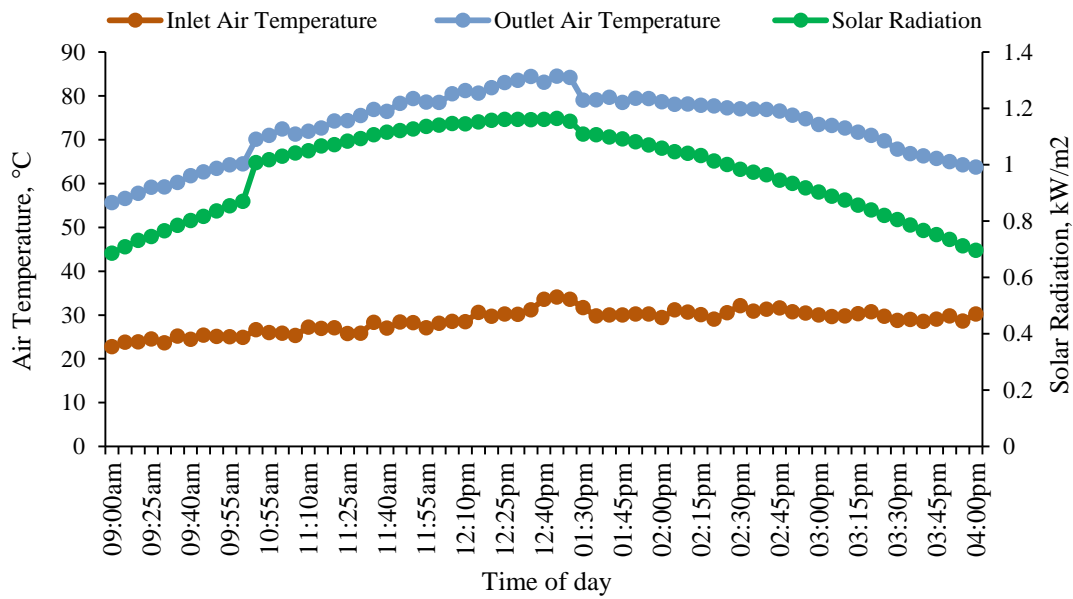


Figure 2 A typical experimental day for solar air heater

The energy efficiency of the solar air heater was calculated using Equation 1:

$$\eta = \dot{m}c_p(T_{out} - T_{in}) / (G_T A_c) \quad (1)$$

Where  $\dot{m}$  is mass flow rate (kg/s),  $c_p$  is specific heat of air (J/kg.K),  $T_{in}$  is inlet temperature (°C),  $T_{out}$  is outlet

temperature (°C),  $G_T$  is solar radiation intensity (W/m<sup>2</sup>) and  $A_c$  is collector surface area (m<sup>2</sup>).

Figure 3 shows energy efficiency for solar air heater. According to Equation 1, energy efficiency calculated and it was found approximately  $\eta=0.25$ .

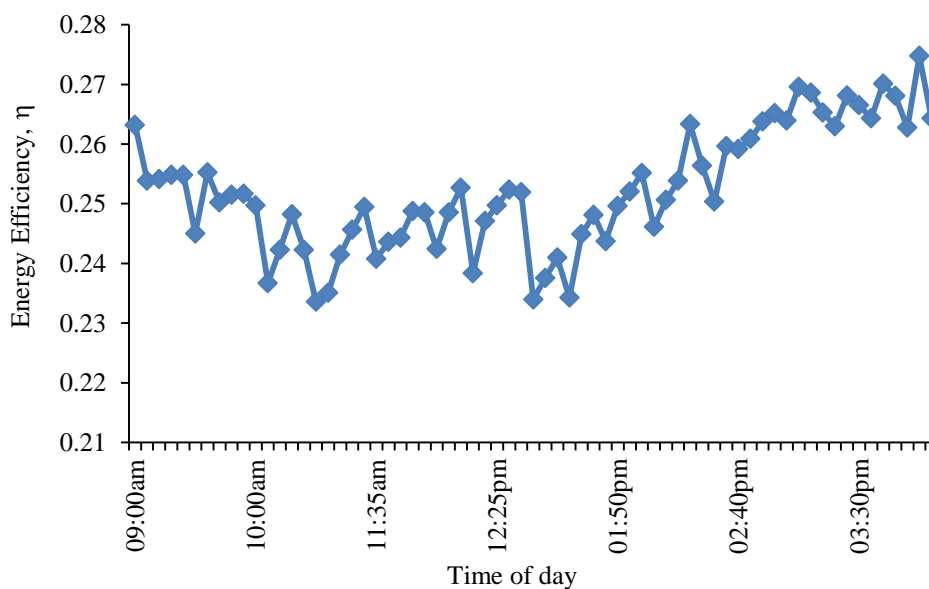


Figure 3 Energy efficiency of the solar air heater.

### 3.1 CFD simulation

ANSYS Release 15.0 software was used for CFD simulations. To gain simulation results using CFD software, a simulation procedure has to be followed. The procedure requires setting the boundary and volume

conditions of the simulated module. Assuming that the collector is a simple flat plate solar air heater, boundaries should have both convection and radiation heat transfer mechanisms. In our system two different convection mechanisms takes place. While natural convection occurs

in the region between glass and absorber plate there is a mixed convection between absorber and bottom plate.

Streamlines in the solar air heater for three different inlet air velocities are shown in Figure4. It seems that, a

circulation zone occurs near the sidewall of the collector and the zone grows with increasing the inlet velocity of air.

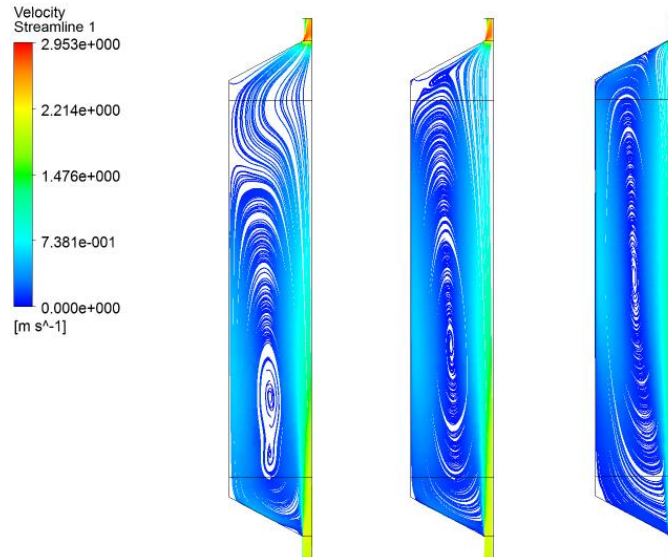


Figure4 Streamlines of air in the solar air heater a)  $v=2$  m/s, b)  $v=3$  m/s, c)  $v=4$  m/s

The effect of inlet air temperature on the outlet temperature were investigated and compared with the experimental data. The comparative data is given on Table 2. Increasing the inlet air temperature causes an increase on the outlet air temperature (Figure5). Table 2

also shows the maximum deviation between the predicted and measured outlet temperature is less than 5%, which means that the accuracy of the numerical analysis is quite acceptable for parametric survey.

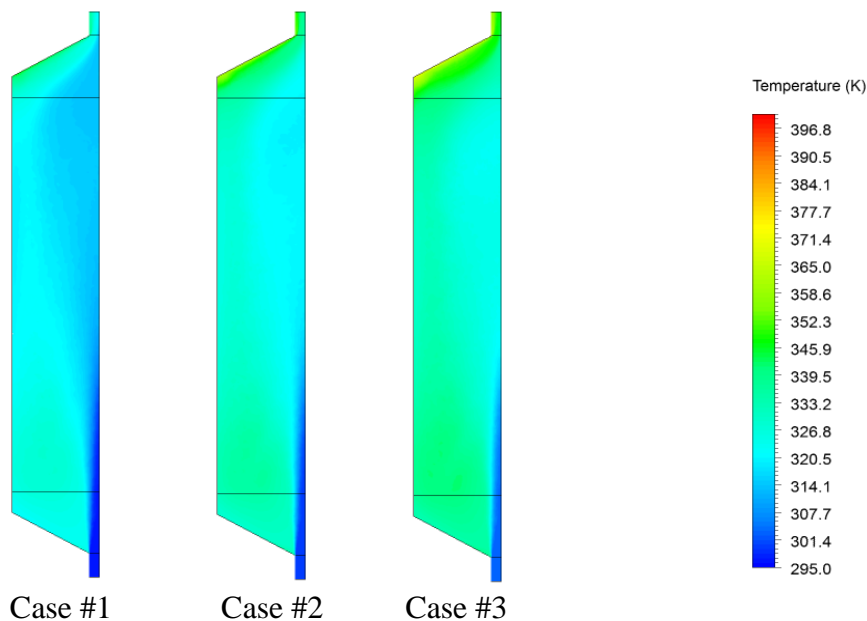


Figure 5 Temperature distribution inside the solar air heater (on  $y = H/2$  plane,  $v=2$ m/s)

**Table 2 Comparison of the experimental and predicted data in terms of outlet air temperature**

Case (#)	Inlet Air Temperature (°C)	Solar Radiation (kW/m <sup>2</sup> )	Experimental Data	Predicted Data	Deviation (%)
			Outlet Air Temperature (°C)	Outlet Air Temperature (°C)	
#1	23.9	0.7312	57.8	55.19	-4.45
#2	26.6	1.0184	70.1	69.74	-0.5
#3	30.2	1.1296	75.8	78.19	3.1

Temperature distributions of air depending on the airflow rate are consistent with the streamlines (Figure6). Solar air collectors can heat up the air much more at the lower air rates, because the air has more time to get hot inside the heater (Alta et al., 2010). As the air velocity increases, the air movement at the edge of the paddle box also increases and the hot air cannot accumulate here. These results also decrease the outlet temperature (Table3). In Figure 7, location of the thermocouples for

given. Temperature values of the defined locations on the absorber plate were also measured from the thermal images. Experimental measurements and the temperature values obtained from thermal images were symbolized as *P* and *M*, respectively. Glass cover was removed before the measurements. The results of the comparison of each five measurements were shown in Figure 8. The difference between the results could be caused from the heat loss while removing the glass cover.

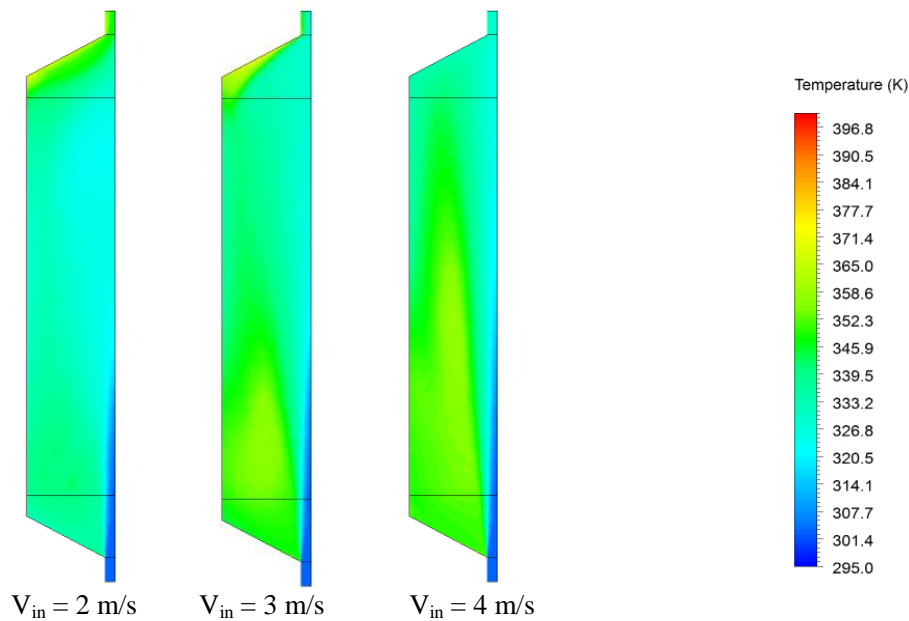


Figure 6 Temperature distribution inside the collector (on  $y = H/2$  plane)

experiments and the results of the thermal images were

**Table 3 Effect of inlet air velocity on the outlet air temperature**

Case (#)	Inlet Air Temperature (°C)	Inlet Air Velocity (m/s)	Solar Radiation (kW/m <sup>2</sup> )	Outlet Air Temperature (°C)
#1		2		78.19
#2	30.2	3	1.1296	64.72
#3		4		56.85

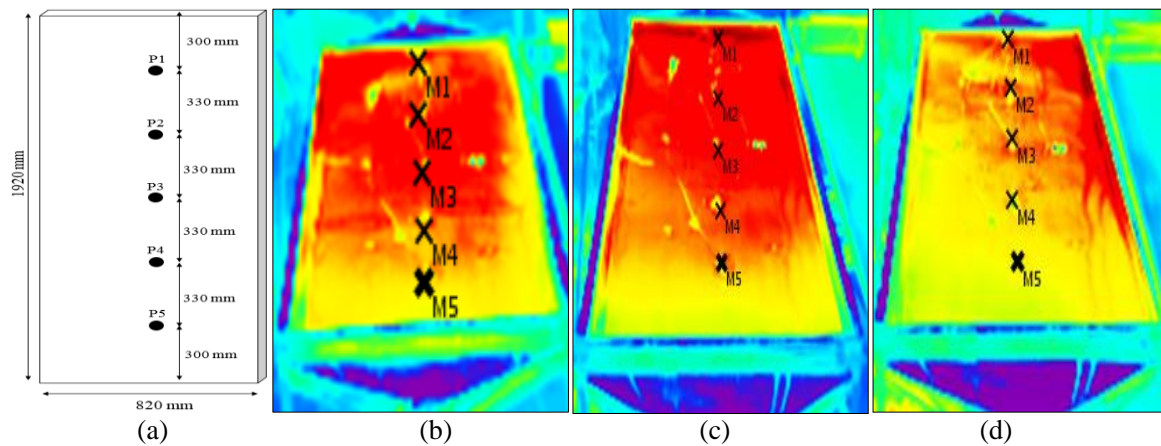


Figure 7 The thermocouple junction placements (P1-P5) (a), thermal images at 10:00 (b), 13:00 (c) and 16:00 (d) on the absorber plate.

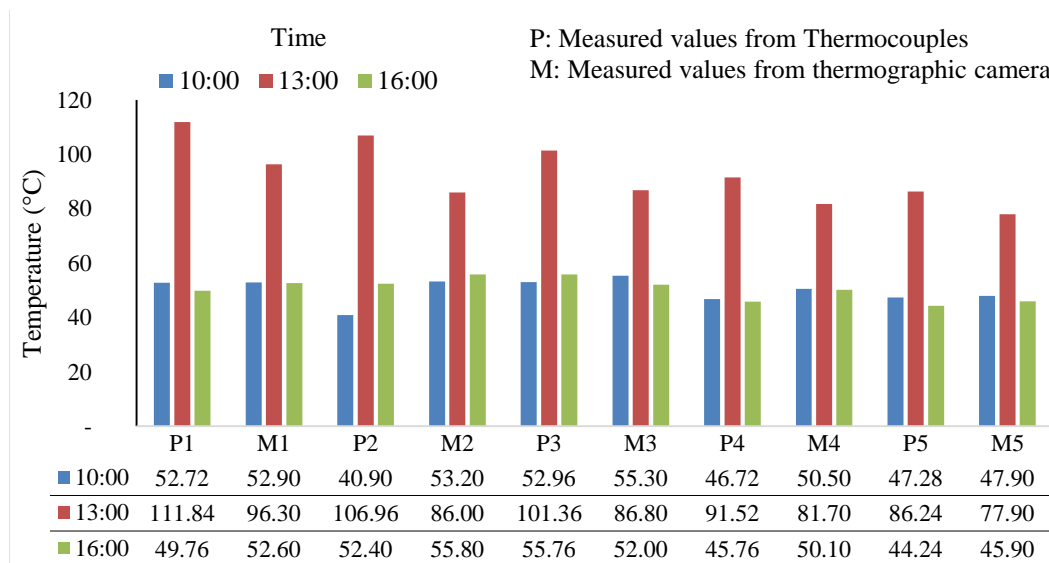


Figure8 Comparison of the temperatures obtained from experimental and thermal images

### 4 Conclusion

In this study, there is a good agreement between the experimental and simulated results for outlet air temperatures. The main conclusions drawn from the results of the present study are given as follows:

- Increasing the inlet air temperature causes an increase in the outlet air temperature,

- Since the heat transfer period increases for lower air flow rates, the outlet temperature increases for lower inlet velocity values,
- Thermographic camera could be used to define the temperatures of locations on the absorber plate.

## References

- Alta, Z.D., E.Bilgili, C.Ertekin, and O. Yaldiz. 2010. Experimental investigation of three different solar air heaters: Energy and exergy analyses. *Applied Energy*, 87(10): 2953-2973.
- Esen, H. 2008. Experimental energy and exergy analysis of a double-flow solar air heater having different obstacles on absorber plates. *Building and Environment*, 43(6): 1046-54.
- Gupta, M.K., and S.C.Kaushik. 2008. Exergy performance evaluation and parametric studies of solar air heater. *Energy*, 33(11): 1691-702.
- Kumar, S., and R.P.Saini. 2009. CFD based performance analysis of a solar air heater duct provided with artificial roughness. *Renewable Energy*, 34(5): 1285-1291.
- Selcuk, M. K. 1977. Solar air heaters and their applications. *Solar energy engineering (A78-27852 10-44)*: 155-82. New York: Academic Press Inc.
- Selmi, M., M.J.Al-Khawaja, and A. Marafia. 2008. Validation of CFD simulation for flat plate solar energy collector. *Renewable Energy*, 33(3): 383-387.
- Yadav, A.S., and J.L.Bhagoria. 2013. Heat transfer and fluid flow analysis of solar air heater: A review of CFD approach. *Renewable and Sustainable Energy Reviews*, 23(2013): 60-79.
- Wang, C., Z. Guan, X. Zhao, and D. Wang. 2006. Numerical simulation study on transpired solar air collector. In: *Proceedings of the sixth international conference for enhanced building operations*, 6-9 November 2006, Shenzhen, China.